Bioorganic & Medicinal Chemistry 19 (2011) 2767–2776

Contents lists available at ScienceDirect

Bioorganic & Medicinal Chemistry

journal homepage: www.elsevier.com/locate/bmc

Introduction of aromatic group on 4′-OH of α-GalCer manipulated NKT cell cytokine production

Wenpeng Zhang [a], Chengfeng Xia [a,b,c,*], Janos Nadas [b], Wenlan Chen [b], Li Gu [a,d], Peng George Wang [a,b,*]

[a] Department of Biochemistry, The Ohio State University, Columbus, OH 43210, USA
[b] Department of Chemistry, The Ohio State University, Columbus, OH 43210, USA
[c] State Key Laboratory of Phytochemistry and Plant Resources in West China, Kunming Institute of Botany, Chinese Academy of Sciences, Kunming, Yunnan 650204, China
[d] State Key Laboratory of Microbial Technology (SKLMT), Shandong University, Jinan, Shandong 250100, China

ARTICLE INFO

Article history:
Received 15 September 2010
Revised 23 November 2010
Accepted 25 November 2010
Available online 2 December 2010

Keywords:
α-GalCer
NKT cell ligand
Computer modeling
CD1d
NKT TCR

ABSTRACT

The glycosphingolipid α-GalCer has been found to influence mammalian immune system significantly through the natural killer T cells. Unfortunately, the pre-clinical and clinical studies revealed several critical disadvantages that prevented the therapeutic application of α-GalCer in treating cancer and other diseases. Recently, the detailed illustration of the CD1d/α-GalCer/NKT TCR complex crystal structural, together with other latest structural and biological understanding on glycolipid ligands and NKT cells, provided a new platform for developing novel glycolipid ligands with optimized therapeutic effects. Here, we designed a series of novel aromatic group substituted α-GalCer analogues. The biological activity of these analogues was characterized and the results showed the unique substitution group manipulated the immune responses of NKT cells. Computer modeling and simulation study indicated the analogues had unique binding mode when forming CD1d/glycolipid/NKT TCR complex, comparing to original α-GalCer.

1. Introduction

As a special sub-population of T cells, natural killer T (NKT) cell expresses a T cell receptor (TCR) that can recognize glycosphingolipids and other glycolipid antigens when they are being presented by antigen presenting cells (APC) through a non-conventional, MHC class I-like glycoprotein named as CD1d.[1–3] NKT cells have a broad influence on immune system due to the varied signals emanating after being stimulated by antigens. Once being activated, the NKT cells will show a reciprocal signal pattern with a rapid but strong secreting of Th1 and Th2 cytokines and other chemokines in a short time period. Through these cytokines and other signal molecules, the NKT cells involve in both innate and adaptive immunity and regulate a broad range of immune responses. As the primary contact between NKT cells and APC, the interaction among NKT TCR, glycolipid antigen and CD1d protein, initiates and affects the outcome of NKT cell immune responses.

CD1d protein is a monomorphic protein and it can present different glycolipid antigens to be recognized by NKT TCR from different individuals, even across species.[4,5] It belongs to the CD1 family, which includes five members in two different classes in human, such as Class I CD1 (CD1a, -b, -c) and Class II CD1 (CD1d and CD1e). There is only a single type of CD1 protein in mouse, CD1d, which is homologous to its human isoform.[6–10]

α-Galactosylceramide (α-GalCer) was originally discovered, and named as agelasphins, by the Pharmaceutical Division of the Kirin Brewery Company during a screen of components derived from marine sponge *Agelas mauritianus* as a reagent to prevent tumor metastases in mice.[11,12] The most striking structural feature of α-GalCer is the α linkage between the sugar and ceramide, which is very uncommon in mammalian systems. Structure–activity relationship (SAR) studies resulted in an optimized ligand, KRN7000, with an 18-carbon sphingosine and a 26-carbon acyl chain.[13] α-GalCer can be readily loaded onto CD1d, and the CD1d/α-GalCer complex on the surface of antigen presenting cells can be recognized by the TCR of all types of NKT cells.[14–16]

α-GalCer has been extensively studied in preclinical studies and clinical trials for treating cancer and various other diseases.[13,15,17–26] However, even the Phase I clinical trials proved that α-GalCer was safe and immune-stimulatory, unfortunately, no optimistic responses in patients have been observed.[27–29]

Several reasons have been indentified to cause the failure of α-GalCer in clinical trial, such as the much lower abundance of NKT cells in human and the ineffectiveness in expanding NKT cells in patients.[27] Also, both the short response period and long term anergy of NKT cells triggered by α-GalCer are not ideal for treating some of the chronic diseases.[27,30–35] The antagonizing effects of

* Corresponding authors. Tel.: +86 871 5223354; fax: +86 871 522 3035 (C.X.); tel.: +1 614 292 9884; fax: +1 614 688 3106 (P.G.W.).
E-mail addresses: xiachengfeng@mail.kib.ac.cn (C. Xia), wang.892@osu.edu, pgwang@chemistry.ohio-state.edu (P.G. Wang).

0968-0896/$ - see front matter © 2010 Published by Elsevier Ltd.
doi:10.1016/j.bmc.2010.11.061

Th1 and Th2 cytokines released after α-GalCer induction is another main factor impaired its clinical effects. So, a further modified α-GalCer analogue with optimized cytokine releasing profile and immune response would have a great therapeutic potential.

The crystal structures of CD1d/α-GalCer complex and CD1d/α-GalCer/NKT TCR complex revealed a great amount of detail information about the interactions among the proteins and glycolipid, which would benefit the new analogue design.[5,36] From the structure, α-GalCer interacts with CD1d and NKT TCR mainly through H-bonds and it maintains the conformation by protruding only -OH groups from galactose ring to the NKT TCR as its lipid tails burying in the CD1d binding groove.

The α-GalCer maintains most of the key interactions with CD1d protein through its ceramide moiety. The 3-OH and 4-OH on the sphingosine chain both form critical H-bonds with CD1d.[36,37] Meanwhile, the glycosidic linkage C1′-O and the C2′-OH on galactose ring are also identified to interact with CD1d protein.[36] An extra H-bond between C3′-OH and CD1d as well as multi van der Waals interactions were also characterized in some of other crystal structures.[37,38]

The α-GalCer interacts with NKT TCR mainly through -OH groups on galactose ring while CDR1α and CDR3α loops of NKT TCR were found to play critical roles. The major interactions include the C2′- and C4′-OH groups forming H-bond with Gly96α, Phe29α and C3′-OH interacting with Ser30α.[5]

The structure–activity relationship study results are consistent with the crystal structure studies. Modifications on sphingosine lipid -OH groups would change the binding affinity but not abolishing the activity of α-GalCer while modifications on C2′- and C3′-OH on galactose ring disrupted the complex and eliminated the activity of α-GalCer due to their critical interactions with CD1d and NKT TCR, also the limited surrounding space.[39–41] The modifications on C6′-OH of galactose ring did not interrupt the interaction inside the complex as it points towards the solvent and surrounded by free space.[42]

For the C4′-OH group, it has been proved that modifications can be tolerated on this group as it is not as critical as the C2′-OH group although it also maintains direct H-bond with NKT TCR in the complex. The modified analogues showed varied immunogenicity against NKT cells depending on the substitution groups.[41,43]

Based on these previous understandings on the interactions among CD1d protein, α-GalCer, and NKT TCR, we designed a series of novel NKT cell ligands with aromatic residues on C4′ of α-GalCer, expecting to introduce π–π stacking effects in the complex and tune immunogenicity against NKT cells through the extra interaction. Here, we are reporting the biological activity tests demonstrated the modifications could manipulate the NKT cell immune response as proposed. The modeling and simulation study revealed the binding affinity change induced by the modification.

2. Results

The new aromatic α-GalCer analogues (structures shown in Fig. 1) were synthesized and characterized as described in Section 5.

2.1. The in vitro stimulation from aromatic glycolipids against NKT hybridoma cells

In the in vitro hybridoma assay, all three analogues showed significant activity against different NKT hybridoma cell lines (DN3A4-1.2, DN3A4-1.4 and N38-2H4) (Fig. 2A). Especially, the compound Ar3-GSL showed an overall stronger stimulation than α-GalCer in all three hybridoma cell lines, which is not common for previous evaluated α-GalCer analogues. Meanwhile, the compounds Ar2-GSL and Ar1-GSL were also showed strong stimulation against certain hybridoma cell lines.

The analogues were presented to stimulate the hybridoma cells directly by surface-bound CD1d protein in the plate-bound CD1d presenting assay. As shown in Figure 2B, for both 1.2 and 2H4 hybridoma cell lines, the compounds Ar1-GSL and Ar3-GSL stimulated stronger hybridoma responses than α-GalCer did, which means the modified analogues Ar1-GSL and Ar3-GSL can be loaded efficiently onto the CD1d protein and bind with NKT TCR with a high binding affinity to trigger a strong NKT hybridoma response.

2.2. The in vivo stimulation profile of aromatic glycolipids

In the splenocytes stimulation assay, all three analogues still showed significant stimulation activity (Fig. 3A). Among the analogues, the compound Ar3-GSL exhibited an overall comparable activity as α-GalCer, especially on Th2 (IL-4) cytokine, which indicated the Ar3-GSL having certain Th2 cytokine preference. The other two analogues are not as active as α-GalCer, except when the stimulation concentration is very high (1000 ng/mL).

To evaluate their in vivo stimulation properties, the blood cytokine profile was characterized after the mice being treated by the analogues. Total 5 μg of each analogues and α-GalCer were iv injected into C57BL/6 mice and the blood sample from each mouse was collected at different time points (0, 2, 4, 6, 12, and 24 h after injection). The cytokine (IFN-γ for Th1; IL-4 for Th2) level in blood serum was characterized by ELISA (Fig. 3B). All the analogues showed a similar time-dependent cytokine stimulation profile as α-GalCer. Specifically, for the Th1 cytokine, the blood IFN-γ concentration reached peak at 12 h after injection. Ar2-GSL and Ar3-GSL reached a stronger Th1 peak than α-GalCer, even they did not show superior stimulation in earlier time points. For the Th2 cytokine, IL-4, Ar3-GSL showed exactly same time profile as α-GalCer, reaching the peak stimulation 2 h after injection and decreasing quickly. Impressively, Ar3-GSL stimulated a much

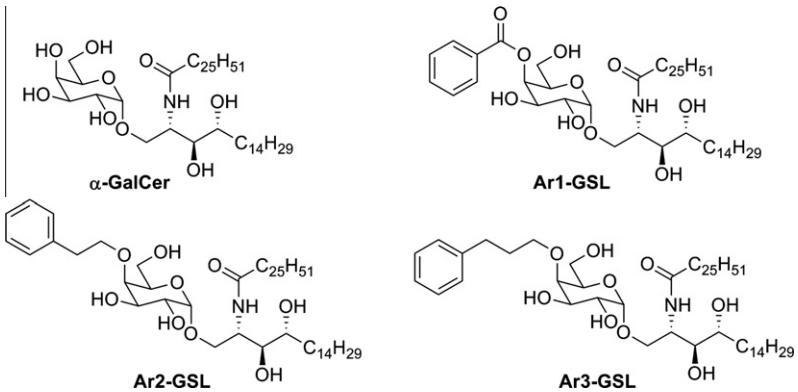

Figure 1. Structures of α-GalCer and novel C4′ aryl-analogues with different length spacer.

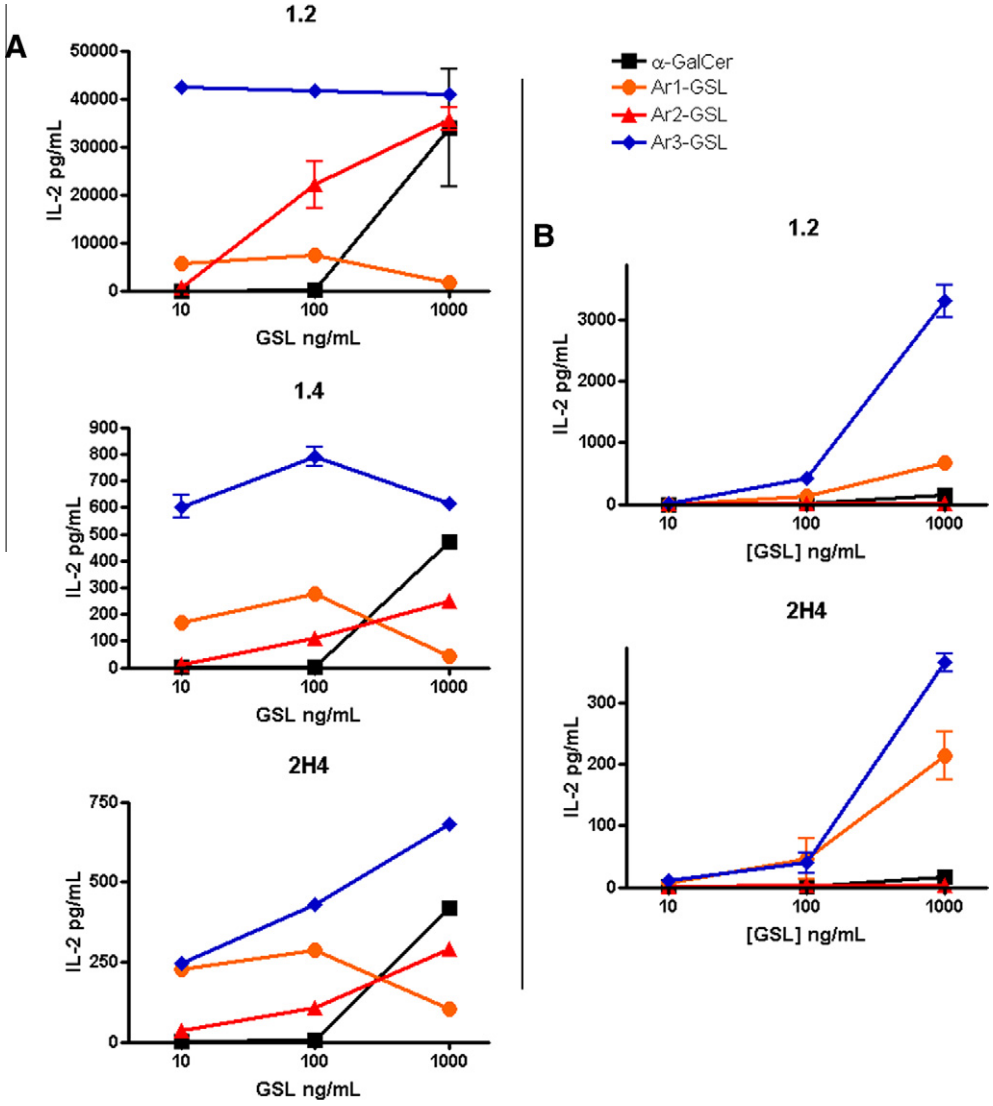

Figure 2. The in vitro hybridoma stimulation by α-GalCer analogues. (A) Three NKT hybridoma cell lines (DN3A4-1.2, DN3A4-1.4, N38-2H4) were stimulated by cell A20/CD1 presented glycolipids. (B) Two NKT hybridoma cell lines (DN3A4-1.2, N38-2H4) were stimulated by plate-bounding CD1d protein presented glycolipids.

stronger Th2 cytokine releasing. For compounds Ar1-GSL and Ar2-GSL, they showed an extended Th2 stimulation peak that maintained a significant Th2 level 4 h after initial injection. These results could be taken as the evidence of manipulated cytokine releasing profile by the C4′ position modification on α-GalCer.

3. Discussion

The information from crystal structure of CD1d/α-GalCer/NKT TCR ternary complex and other related complexes, together with the results from in vitro and in vivo biological studies, has showed an insight into the recognition interactions between the glycolipid antigen and involved functional proteins, especially the interactions among the galactose sugar ring, TCR CDR loops, and CD1d protein. Both the C2′- and C3′-OH groups forms critical H-bonds with residues from CDR1α and CDR3α loops of NKT TCR and CD1d protein. Most of the modifications on these two -OH groups would abolish the H-bonds, change the binding orientation of ligand and receptor, and overall eliminate the immunogenicity of resulted ligands.[5,44] On the other hand, the modification on the C4′-OH resulted a series of analogues with activity profiles varied in a spectrum. The crystal structure also shows, although it forms an H-bond with CDR1α loop, the C4′-OH itself, like the C6′-OH, appears to be located in a much more open solvent-accessible cavity, comparing to the buried position of C2′- and C3′-OH.[5,41,43]

The crystal structure revealed the presence of two aromatic residues around the C4′-OH position, Phe51α of TCR and Trp153 of CD1d,[5] which suggests the possibility of incorporating π–π stacking interactions to increase the binding of glycolipid ligand to both CD1d and TCR. To validate this hypothesis, the homology models of several C4′ position aromatic modified α-GalCer analogues were created mainly based on the CD1d/α-GalCer/NKT TCR ternary structure. Based on our previous study,[45] the computer simulation results confirmed the possibility of forming π–π stacking between the aromatic rings from Phe51α and proposed C4′ aromatic α-GalCer analogues while no such interaction was predicted for the aromatic ring from Trp153 of CD1d protein,[45] which may be beneficial for avoiding too much conformation disrupt from the extra interaction.

Previous results illustrated that the presence of a bulky group on the C4′ position will abolish the immunogenicity, and the antigen can be recognized by the NKT TCR only after the bulky group being removed by glycosidase.[5,41,43] The biological activity study

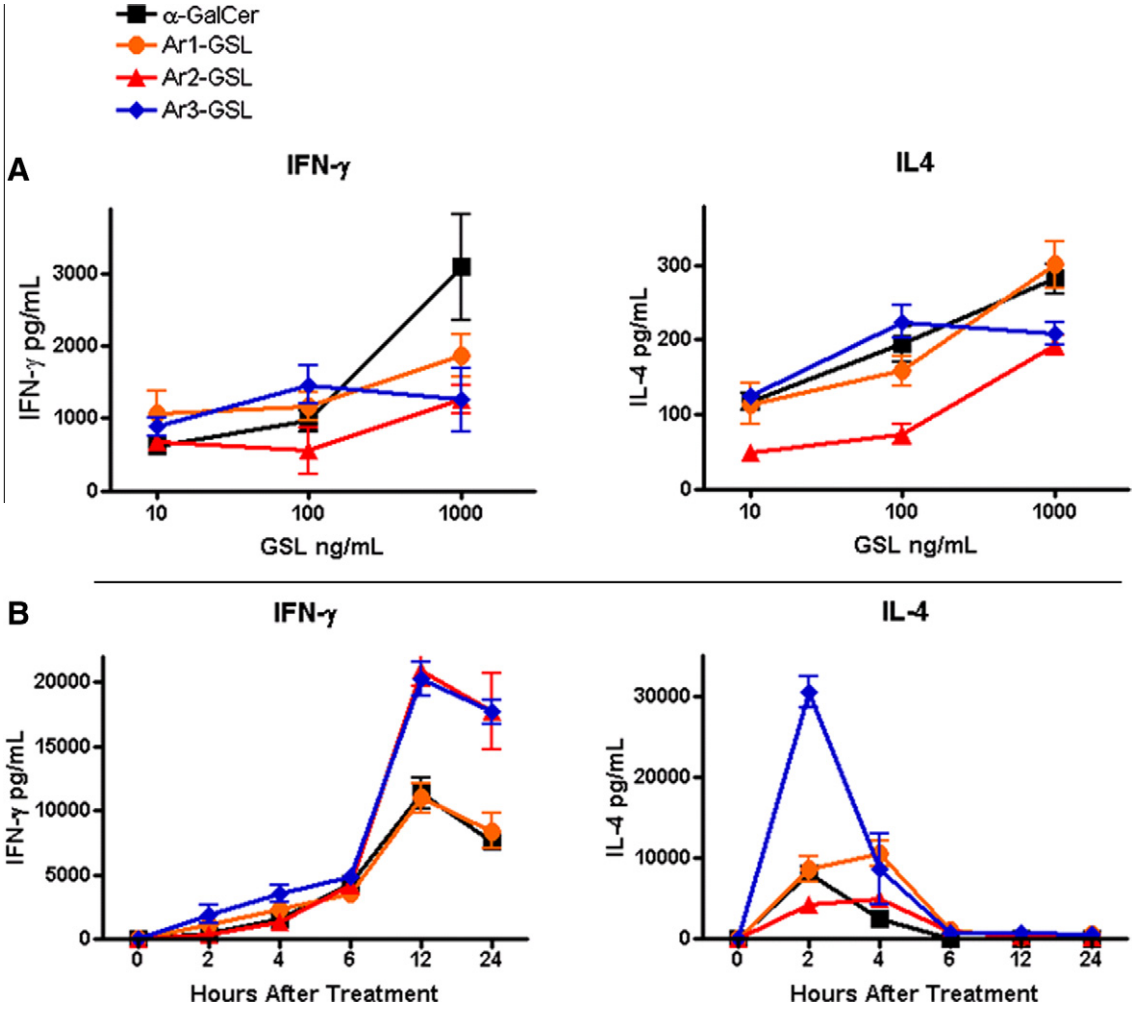

Figure 3. The in vivo immunogenicity profile of aromatic α-GalCer analogues. (A) The cytokines (IFN-γ, IL-4) released by mouse splenocytes after being stimulated by glycolipid antigens. (B) The time dependent pattern of cytokine (IFN-γ, IL-4) level in mouse serum after iv treatment of glycolipids.

proved that these aromatic analogues do have the immunogenicity against the NKT cells. As all of the analogues showed significant activity in varied assays, it means the introducing of aromatic rings onto the C4′ position of α-GalCer did not interrupt the basic binding and recognition among the glycolipid ligand, CD1d and NKT TCR.

Through the data, it can be found that the aromatic substitution at the C4′ of α-GalCer affected the NKT cell function by altering the binding affinity with CD1d and NKT TCR while the substitution still kept the interactions strong enough for NKT cell stimulation. Both the in vitro hybridoma stimulation and plate-bound CD1d presenting assay indicated the differences of cytokine releasing strength, which is resulted by the different binding affinity that induced by the aromatic modification groups. Especially in the plate-bound CD1d presenting assay, the binding affinity would be the main factor causing the stimulation variations since the affects from the antigen presenting cells were excluded by presenting the ligands directly through plate-binding CD1d protein. As all the analogues share a same ceramide moiety and the C4′-OH on α-GalCer mainly interacts with NKT TCR, the loading efficiency for each analogue onto CD1d should also be similar. This means the hybridoma responses level of plate-bound CD1d presenting assay was majorly determined by the binding strength between the presented ligands and NKT TCR, which was affected by the modification on C4′ group in this case. For example, comparing to the very active compound Ar3-GSL which has a 3-carbon linker between C4′-O and the aromatic ring, the compound Ar2-GSL with a 2-carbon linker only showed very limited stimulation. This indicates a correct linker length for the aromatic ring to locate properly is very critical. Meanwhile, the significant stimulation from the single-carbon linker compound Ar1-GSL should be partly credited to the compensation binding affinity from the extra carbonyl group on the linker carbon.

In the in vivo splenocytes culture, the aromatic analogues showed stimulation effects on both Th1 (IFN-γ) and Th2 (IL-4) cytokines, but, with weaker relative stimulation strength from the hybridoma model and plate-bound CD1d presenting model, comparing to the stimulation strength from α-GalCer. Among the analogues, the compound Ar3-GSL is still superior to the others, with the compound Ar1-GSL following, and then the compound Ar2-GSL, which is consistent with the plate-bound CD1d presenting assay results. This result can be also taken as evidence that the in vivo stimulation profile of NKT cell is related to the binding property between glycolipid ligand and NKT TCR. The preference of Th1 and Th2 cytokines for these analogues had not much difference from the α-GalCer although the analogues showed a slight Th2 preference comparing the relative strength against α-GalCer.

In the in vivo mouse stimulation, the analogue compounds gave a similar blood Th1 cytokine (IFN-γ) profile as α-GalCer did, although with strength variations, when some of the analogues

changed significantly on the profile of Th2 cytokine (IL-4) (Fig. 3B). The compound Ar3-GSL showed the most significant IL-4 stimulation while the time pattern is still same as α-GalCer's. The compounds Ar1-GSL and Ar2-GSL both gave a lower but broader peak which indicates they extended the stimulation retention on Th2 cytokine. This could be caused by the changed metabolism process of the analogues due to the modification, or, by the binding affinity change, which is more reasonable here as the both analogues did not show time dependent profile change on Th1 cytokine.

Molecular modeling and simulation were also applied to further characterize the interaction among ligands and proteins. Since the first crystal structure of CD1d/NKT TCR complex (2PO6) was published, five more crystal structures have been solved with mCD1d or varying the chains of NKT TCR. All the crystal structures showed a similar binding footprint implying that the interaction between CD1d and TCR is more of a lock-and-key interaction rather than an induced-fit interaction.[46] A 3D alignment of all the crystal structures verified this observation. More importantly, different ligands were shown to induce small conformational changes in TCR upon TCR binding to ensure that the correct binding footprint would be formed, and that these minor changes could potentially explain the weaker potency of the ligands.[46]

Molecular dynamics simulations were used to determine the cause in the varying cytokine profiles of the different ligands of α-GalCer, Ar1-GSL, Ar2-GSL, and Ar3-GSL. The experimental procedures utilized mCD1d to present the four ligands to NKT-TCR. Therefore, a new model had to be created to analyze the experimental results since no crystal structure exists of mCD1d bound to the human NKT-TCR protein possessing the NKT15α and β chains. The difference between mCD1d and hCD1d as well as their respective NKT-TCR proteins has everything to do with the lack of aromatic residues lying posterior to the 4′-OH of α-GalCer (Fig. 4). The new model possessed the Phe51α on the CDR loop directly above α-GalCer but lacked the Trp153 amino acid on CD1d directly below the 4′-OH of α-GalCer. This model underwent an energy minimization followed by the modification of the α-GalCer ligand to yield Ar1-GSL, Ar2-GSL, and Ar3-GSL and then a subsequent minimization. The two complexes of mCD1d/Ar2-GSL and Ar3-GSL/TCR then underwent a 200 picosecond molecular dynamics simulation in implicit solvent to see whether any conformational changes could be induced by different 4′- substituents.

The molecular dynamics simulations were able to show minute conformational changes that can potentially explain the varying cytokine profiles of Ar2-GSL and Ar3-GSL (Fig. 5). The 2 carbon linker on Ar2-GSL is just flexible and long enough to form the predicted π–π stacking interactions with Phe51α. On the other hand, the 3 carbon linker of Ar3-GSL creates a length that is too long to interact with Phe51α, and its presence only displaces Phe51α slightly from its crystal conformation. All the hydrogen bonds between the ligands and the two proteins are maintained, therefore, the added non-covalent π–π interaction should add to the binding energy in the complex. Non-covalent π–π interactions have been shown to have binding energies of 1–3 kcal/mol with substituents on the aromatic rings being able to increase binding energies by 1 kcal/mol.[47] However, the experimental results show that Ar3-GSL is a more potent ligand than Ar2-GSL.

The early computational studies performed in our laboratory showed that different ligands were capable of inducing slight changes in the binding footprint of CD1d and TCR.[45] The binding footprint of Ar2-GSL was found to possess very small differences from Ar3-GSL even after only the 200 ps simulation (Fig. 5). The Tyr48β lost its hydrogen bond with Glu83 on CD1d more than

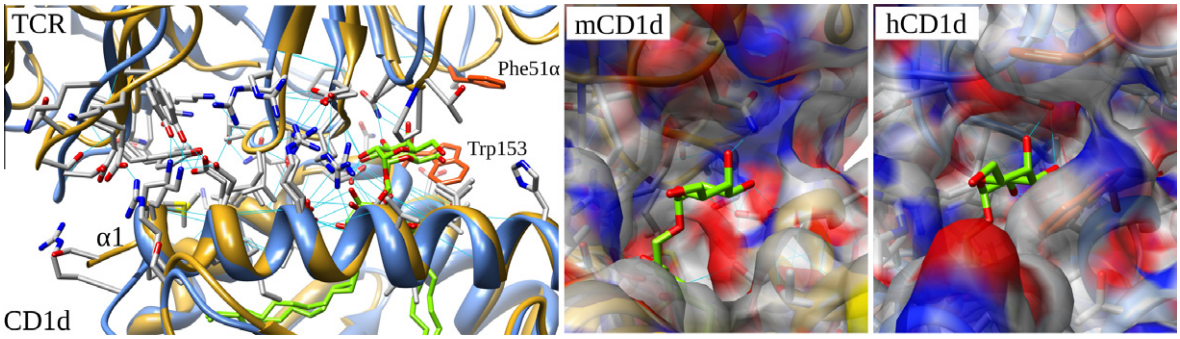

Figure 4. The aligned crystal structures of mCD1d and hCD1d presenting α-GalCer to their respective NKT-TCR proteins, PDB ID 3HE6 and 2PO6, respectively. The major difference between the two crystal structures lies in the fact that the mCD1d structure lacks both aromatic residues that sit behind the 4′-OH position of α-GalCer. The surface area representation of hCD1d shows that there may be enough space between the residues for potential interactions with a substituent group on the 4′-position.

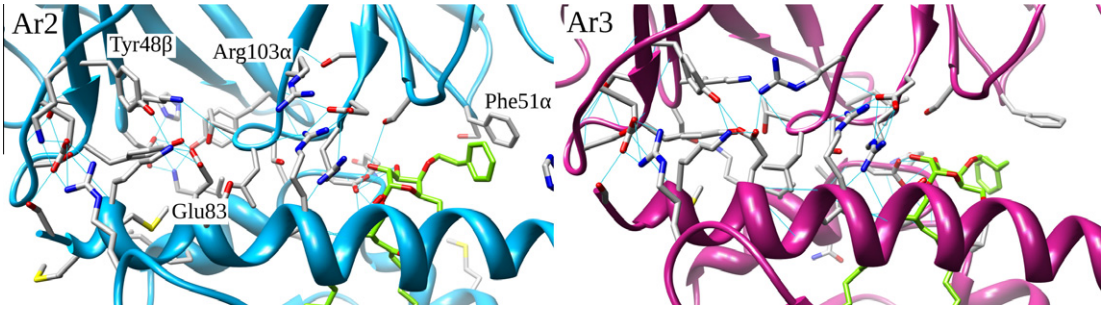

Figure 5. The binding footprints of Ar2-GSL and Ar3-GSL complexes after 200 ps of molecular dynamics simulations. The two-carbon linker on Ar2-GSL provides enough flexibility and length to form π–π interactions with Phe51α, whereas in Ar3-GSL, the three-carbon linker is too long. However, the slight displacement of TCR for both ligands causes the loss of hydrogen bonds involving Glu83 for Ar2-GSL or the maintaining and formation of new hydrogen bonds involving Glu83 for Ar3-GSL. The breaking and forming of such non-covalent interactions between the two proteins is a possible explanation for the potency of the ligands.

likely due to a tilting upward of TCR upon formation of the π–π interaction. For Ar3-GSL, this hydrogen bond was maintained as well as Arg103α swinging over to form an additional hydrogen bond with Glu83. The gaining of the π–π non-covalent interaction can not compensate for the loss of a hydrogen bond since each hydrogen bond will contribute between 2 and 7 kcal/mol energy to the overall binding energy.[48] Since both compounds are still capable of eliciting a cytokine response, the binding footprint has to be maintained for both. The difference in their cytokine profiles though will more than likely be due to slight changes in the TCR protein upon binding causing the breaking or formation of novel non-covalent interactions.

This result would further extend the understanding on how the binding affinity between CD1d presented glycolipid ligands and NKT TCR could affect the NKT cell response. The recognition and binding affinity between sugar moiety of glycolipid ligand and NKT TCR could affect the NKT cell response pattern as it would affect the stability of CD1d/glycolipid/NKT TCR complex. The overall in vivo effects on NKT cell response include the response strength and also the cytokine preference. Moreover, it also includes the time profile of NKT cell response as the modification on the analogues could not only change the space fitting and binding strength, but also the time-dependent manipulation of binding partners' on-and-off ratio.

In summary, we developed and synthesized a novel type of glycolipid ligands with the help from previous understandings on structure and activity properties. From the new group analogues, we further illustrated how the structure of glycolipid ligands, especially the sugar moiety, would affect the NKT cell immune response. The introducing of aromatic group on the C4′ position with suitable linker does not block the NKT TCR recognizing ligand. Instead, it increased the interaction affinity of ligand with NKT TCR by π–π stacking and thus changed the profile of cytokine releasing both in strength and time-dependence. These results provide a new understanding of NKT response and give some guide on the future utility of glycosphingolipids in clinical trials.

4. Conclusion

We designed and synthesized a series of aromatic modified α-GalCer analogues. The biological activity study proved the immunogenicity of these novel analogues. Our results also showed the π–π stacking effects introduced by the aromatic substitution group altered the immunogenicity profile of α-GalCer, which could help to explore the potential therapeutic application of glycolipids.

5. Experiment and materials

5.1. General information for cell culture and compounds synthesis

All solvents were dried with solvent-purification system from Innovative Technology, Inc. All reagents were obtained from commercial sources and used without further purification. Analytical TLC was carried out on Silica Gel 60 F254 aluminum-backed plates (E. Merck). The 230–400 mesh size of the same absorbent was utilized for all chromatographic purifications. ^{1}H and ^{13}C NMR spectra were recorded at the indicated field strengths. The high-resolution mass spectra were collected at The Ohio State University Campus Chemical Instrumentation Center.

The A20/CD1cell and hybridoma cells[49,50] are maintained in RPMI-1640 (Gibco, CA, USA) with 10% FBS (Gibco, CA, USA) and antibiotics. The cell culture was always maintained in a CO_2 incubator at 37 °C with 5% CO_2. The synthetic glycolipid compounds were dissolved in DMSO as stock solution and then diluted with medium to the indicated working concentrations.

5.2. Preparation of the ceramide acceptor

5.2.1. (2*S*,3*S*,4*S*)-2-Azido-octadecan-1,3,4-triol (2)

As shown in Scheme 1, to a mixture solution of CH_2Cl_2 (5 mL) and H_2O (5 mL) containing NaN_3 (2.05 g, 31.5 mmol) cooled at 0 °C was added dropwise of Tf_2O (1.1 mL, 6.3 mmol) in 20 min. After addition the resulting mixture was continued stirring for 3 h. The organic layer was separated and the aqueous was extracted with CH_2Cl_2 (2 × 2 mL). The combined organic layer was washed with saturated Na_2CO_3 aqueous.

To a suspension of phytosphingosine **1** (1.0 g, 3.1 mmol), K_2CO_3 (2.18 g, 15.8 mmol) and Cu_2SO_4 (20 mg) in a mixture of MeOH (4 mL) and H_2O (3 mL) were added the above organic layer which contained TfN_3. More MeOH was added to make the mixture to be a homogenous solution. The reaction mixture was stirred overnight at room temperature. The organic solvent was removed in vacuo. The aqueous was extracted with ethyl acetate. After dried over anhydrous Na_2SO_4, it was purified by silica gel flash chromatography (1:1 EtOAc–hexane) to give 0.96 g of product **2** in 89% yield. ^{1}H NMR (400 MHz, $CDCl_3$): δ 4.02 (dd, J = 11.6, 5.2 Hz, 1H), 3.92 (dd, J = 11.6, 4.4 Hz, 1H), 3.82 (m, 1H), 3.78 (m, 1H), 3.69 (m, 1H), 1.64–1.54 (m, 3H), 1.46–1.28 (m, 23H), 0.91 (t, J = 6.8 Hz, 3H); ^{13}C NMR (100 MHz, $CDCl_3$): δ 74.8, 72.6, 63.4, 62.0, 32.0, 31.9, 29.6, 29.5, 29.3, 25.7, 22.6, 14.0.

5.2.2. (2*S*,3*S*4*S*)-2-Azido-3,4-di-*O*-benzyl-octadecan-1,3,4-triol (3)

A solution of azido-sphingosine **2** (0.40 g, 1.2 mmol), trityl chloride (1.3 g, 4.7 mmol) and catalytic amount of DMAP in dry pyridine (5 mL) was stirred at 50 °C for 10 h. The reaction mixture was diluted with CH_2Cl_2, and washed with cooled 1 N HCl, saturated aqueous $NaHCO_3$ and brine. The organic layer was dried over anhydrous Na_2SO_4 and concentrated. The residue was then dissolved in dry DMF (6 mL) and then treated with 60% NaH (106 mg, 2.6 mmol) for 10 min. BnCl (0.30 mL, 2.6 mmol) was added by syringe and the reaction was stirred overnight. After the solvent was removed in vacuo, the residue was dissolved in water, extracted with ethyl ether. The organic extraction was concentrated and then dissolved in a mixture of CH_2Cl_2 and MeOH (2:1, 9 mL). pTsOH·H_2O (95 mg, 0.5 mmol) was added and the reaction was stirred for 1 h at room temperature. After concentrated, the residue was purified by silica gel flash chromatography (1:6 EtOAc–hexane) to give 0.43 g of acceptor **3** in 68% yield for three steps. ^{1}H NMR (500 MHz, $CDCl_3$): δ 7.37–7.28 (m, 10H), 4.73 (d, J = 11.3 Hz, 1H), 4.69 (d, J = 11.3 Hz, 1H), 4.65 (d, J = 11.4 Hz, 1H), 4.59 (d, J =11.4 Hz, 1H), 3.92 (dd, J = 11.7, 5.1 Hz, 1H), 3.82 (dd, J = 11.7, 5.1 Hz, 1H), 3.73 (m, 1H), 3.70 (m, 1H), 3.66 (m, 1H), 1.71 (m, 1H), 1.59 (m, 1H), 1.45 (m, 1H), 1.37–1.27 (m, 23H), 0.91 (t, J = 6.8 Hz, 3H); ^{13}C NMR (125 MHz, $CDCl_3$): δ 138.0, 137.7, 128.6, 128.5, 128.1, 128.03, 128.0, 127.9, 80.5, 79.0, 73.7, 72.6, 63.1, 62.3, 32.0, 30.3, 29.7, 29.68, 29.6, 29.59, 29.4, 25.5, 22.7, 14.1.

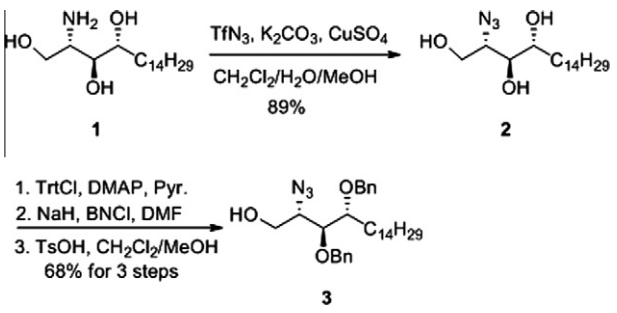

Scheme 1. Preparation of the ceramide acceptor.

5.3. Preparation of 4-hydroxyl glycolipid

5.3.1. 2,3-Di-*O*-benzyl-4,6-*O*-benzyliden-α-D-galactopyranosyl-(1,1)-(2*S*,3*S*,4*R*)-2-azido-3,4-di-*O*-benzyl-octadecan-1,3,4-triol (5)

As shown in Scheme 2, Powered 4 Å molecule sieves (3.0 g) were added to a stirred solution of benzylidene protected trichloroacetimide donor **4** (1.25 g, 2.10 mmol) and azido lipid **3** (1.00 g, 1.91 mmol) in fresh dried CH_2Cl_2 (20 mL). After 30 min, the mixture was cooled to −40 °C, TMSOTf (57 μL, 0.27 mmol) was added by syringe and the resulting mixture was stirred for 2 h. The reaction was quenched by addition of Et_3N (0.2 mL), and the mixture was filtered through Celite pad. The filtered was concentrated and purified by column chromatography with hexane/ethyl acetate (8:1) to give 1.35 g of product in 74% yield. ^1H NMR (500 MHz, $CDCl_3$) δ 7.56–7.24 (m, 25H), 5.48 (s, 1H), 5.00 (d, J = 3.4 Hz, 1H), 4.89 (d, J = 11.8 Hz, 1H), 4.84 (d, J = 12.4 Hz, 1H), 4.77 (d, J = 12.4 Hz, 1H), 4.70 (d, J = 12.1 Hz, 1H), 4.69 (d, J = 11.3 Hz, 1H), 4.64 (d, J = 11.6 Hz, 1H), 4.61 (d, J = 11.8 Hz, 1H), 4.53 (d, J = 11.6 Hz, 1H), 4.19 (d, J = 3.2 Hz, 1H), 4.13 (dd, J = 10.3, 3.4 Hz, 1H), 4.10 (d, J = 11.5 Hz, 1H), 4.06 (dd, J = 10.4, 3.3 Hz, 1H), 4.03 (d, J = 7.9 Hz, 1H), 3.91 (d, J = 12.0 Hz, 1H), 3.78–3.72 (m, 3H), 3.66 (m, 1H), 3.60 (br, 1H), 1.70 (m, 1H), 1.57 (m, 1H), 1.44 (m, 1H), 1.34–1.25 (m, 23H), 0.92 (t, J = 6.9 Hz, 3H); ^{13}C NMR (125 MHz, $CDCl_3$) δ 138.8, 138.4, 138.1, 137.9, 128.9, 128.4, 128.38, 128.3, 128.2, 128.1, 127.9, 127.8, 127.78, 127.73, 127.70, 127.6, 127.5, 127.48, 126.4, 101.1, 99.2, 79.5, 79.0, 75.9, 75.5, 74.7, 73.8, 73.5, 72.1, 72.0, 69.4, 68.5, 63.0, 61.7, 31.9, 30.1, 29.8, 29.7, 29.68, 29.66, 29.6, 29.4, 25.5, 22.7, 14.1; HRMS calcd for $C_{59}H_{75}N_3O_8Na$ ([M+Na]$^+$) 976.5446, found 976.5467.

5.3.2. 2,3,6-Tri-*O*-benzyl-α-D-galactopyranosyl-(1,1)-(2*S*,3*S*,4*R*)-2-azido-3,4-di-*O*-benzyl-octadecan-1,3,4-triol (6)

Powered 4 Å molecular sieves (0.5 g) were added to a stirred solution of compound **5** (395 mg, 0.41 mmol) in freshly dried CH_2Cl_2 (5 mL). After 30 min, the mixture was cooled to −78 °C, Et_3SiH (0.20 mL, 1.24 mmol) and TfOH (72 μL, 0.82 mmol) were added by syringes respectively. The reaction mixture was stirred for 2 h at −78 °C and then was quenched by addition of solid $NaHCO_3$ (0.5 g) and MeOH (1 mL). The mixture was allowed to warm to room temperature and filtered through a Celite pad. The solids were washed three times with CH_2Cl_2. The combined filtrates were washed with saturated aqueous $NaHCO_3$ and brine. After dried over anhydrous Na_2SO_4, filtered and concentrated, the residue was purified by column chromatography with hexane/ethyl acetate (5:1) to give 368 mg of product as colorless oil in 94% yield. ^1H NMR (500 MHz, $CDCl_3$) δ 7.42–7.25 (m, 25H), 4.94 (d, J = 2.8 Hz, 1H), 4.82 (d, J = 11.7 Hz, 1H), 4.81 (d, J = 12.0 Hz, 1H), 4.75 (d, J = 11.7 Hz, 1H), 4.71 (d, J = 12.4 Hz, 1H), 4.70 (d, J = 11.5 Hz, 1H), 4.67 (d, J = 11.4 Hz, 1H), 4.61 (d, J = 11.6 Hz, 1H), 4.59 (d, J = 11.9 Hz, 1H), 4.55 (d, J = 12.2 Hz, 1H), 4.53 (d, J = 11.6 Hz, 1H), 4.10 (m, 1H), 4.08 (dd, J = 10.3, 1.9 Hz, 1H), 3.97 (t, J = 5.9 Hz, 1H), 3.95 (m, 2H), 3.80–3.75 (m, 3H), 3.72 (m, 1H), 3.68–3.64 (m, 2H), 2.67 (br, 1H), 1.70 (m, 1H), 1.58 (m, 1H), 1.44 (m, 1H), 1.36–1.25 (m, 23H), 0.93 (t, J = 6.7 Hz, 3H); ^{13}C NMR (125 MHz, $CDCl_3$) δ 138.6, 138.5, 138.2, 138.16, 138.0, 128.5, 128.4, 128.37, 128.35, 128.3, 127.9, 127.8, 127.7, 127.68, 127.6, 98.4, 79.4, 79.1, 77.5, 75.7, 73.8, 73.6, 73.2, 72.6, 72.0, 69.6, 68.9, 68.1, 68.1, 62.0, 32.0, 30.0, 29.8, 29.74, 29.72, 29.70, 29.68, 29.65, 29.4, 25.4, 22.7, 14.2; HRMS calcd for $C_{59}H_{77}N_3O_8Na$ ([M+Na]$^+$) 978.5603, found 978.5589.

5.4. Preparation of Ar1-GSL

5.4.1. 4-*O*-Benzoyl-2,3,6-tri-*O*-benzyl-α-D-galactopyranosyl-(1,1)-(2*S*,3*S*,4*R*)-2-azido-3,4-di-*O*-benzyl-octadecan-1,3,4-triol (7)

As shown in Scheme 3, to a solution of alcohol **6** (80 mg, 0.084 mmol), Et_3N (19 μL, 0.14 mmol) and catalytic amount of DMAP in dry CH_2Cl_2 (2 mL) was added BzCl (14 μL, 0.12 mmol). The resulting mixture was stirred for 3 h at room temperature and then diluted with CH_2Cl_2 (10 mL), washed with brine. The organic layer was dried over anhydrous Na_2SO_4, filtered and concentrated in vacuo. The residue was purified by column chromatography with hexane/ethyl acetate (12:1) to give 82 mg of product in 92% yield. ^1H NMR (500 MHz, $CDCl_3$) δ 8.06 (d, J = 7.5 Hz, 2H), 7.61 (t, J = 7.4 Hz, 1H), 7.48 (t, J = 7.7 Hz, 2H), 7.38–7.22 (m, 25H), 5.88 (d, J = 2.1 Hz, 1H), 5.01 (d, J = 3.3 Hz, 1H), 4.89 (d, J = 11.4 Hz, 1H), 4.84 (d, J = 10.0 Hz, 1H), 4.73–4.60 (m, 6H), 4.53 (d, J = 11.4 Hz, 1H), 4.51 (d, J = 11.6 Hz, 1H), 4.41 (d, J = 11.9 Hz, 1H), 4.24 (t, J = 6.2 Hz, 1H), 4.16 (dd, J = 10.1, 3.1 Hz, 1H), 4.11 (d, J = 9.3 Hz, 1H), 3.97 (dd, J = 10.0, 3.4 Hz, 1H), 3.83–3.78 (m, 3H), 3.65 (m, 1H), 3.54 (d, J = 6.3 Hz, 2H), 1.70 (m, 1H), 1.58 (m, 1H), 1.44 (m, 1H), 1.37–1.26 (m, 22H), 0.93 (t, J = 6.8 Hz, 3H); ^{13}C NMR (125 MHz, $CDCl_3$) δ 165.8, 138.6, 138.5, 138.2, 137.8, 133.0, 130.1, 129.9, 128.38, 128.37, 128.34, 128.25, 128.21, 127.92, 127.91, 127.87, 127.76, 127.70, 127.64, 127.61, 127.5, 127.4, 98.9, 79.4, 79.0, 76.2, 75.2, 73.8, 73.6, 73.5, 72.0, 71.8, 68.8, 68.7, 68.5, 61.9, 32.0, 30.0, 29.8, 29.74, 29.72, 29.70, 29.68, 29.66, 29.4, 25.4, 22.7, 14.2; HRMS calcd for $C_{66}H_{81}N_3O_9Na$ ([M+Na]$^+$) 1082.5865, found 1082.5829.

5.4.2. Ar1-GSL

Triphenylphosphine (12 mg, 0.045 mmol) was added to a solution of azide **7** (42 mg, 0.039 mmol) in benzene (3 mL) and water (0.1 mL). The reaction mixture was stirred at 50 °C for 10 h. The

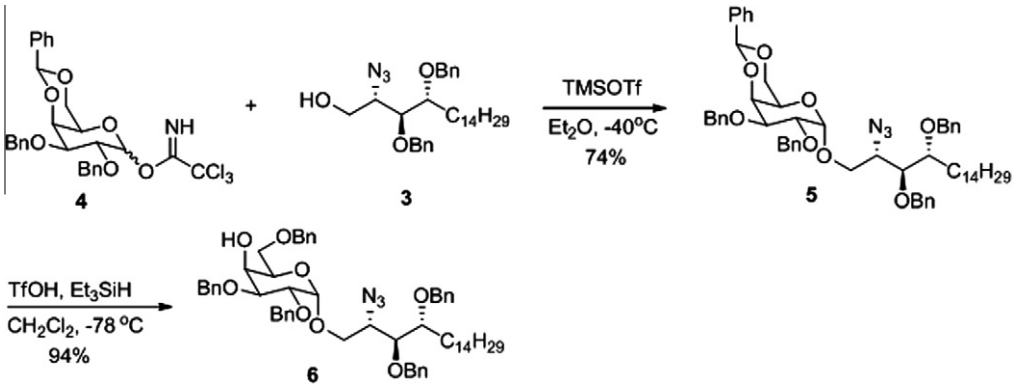

Scheme 2. Preparation of 4-hydroxyl glycolipid.

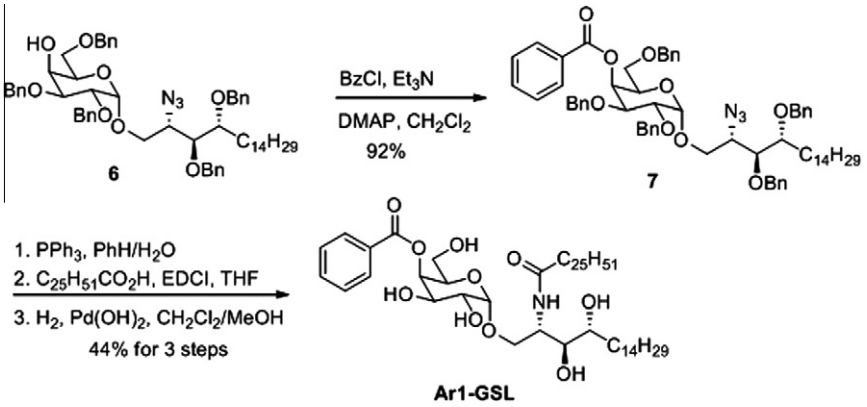

Scheme 3. Preparation of Ar1-GSL.

solvent was evaporated under reduced pressure and azeotroped with benzene (2 × 10 mL). Then it was dissolved in dry THF (2 mL) and treated with cerotic acid (18 mg, 0.045 mmol) and EDCI (9 mg, 0.047 mmol). After stirring for 10 h at room temperature, the solvent was evaporated and the residue was partitioned between CH_2Cl_2 (10 mL) and water (10 mL). The organic layer was separated and dried over Na_2SO_4. After concentrated, the residue was purified by silica gel flash chromatography (1:3 EtOAc–hexane) to provide 34 mg as foam.

A suspension of the above product (34 mg, 0.024 mmol) and 5 mg of $Pd(OH)_2$ in $EtOH/CH_2Cl_2$ (3:1, 3 mL) was shaken for 4 h under H_2 atmosphere (40 psi). The catalytic Pd/C was filtered off through a Celite pad and the filtrate was concentrated to give 18 mg of product in 44% yield as powder. HRMS calcd for $C_{57}H_{103}NO_{10}Na$ ($[M+Na]^+$) 984.7474, found 984.7502.

5.5. Preparation of Ar2-GSL

5.5.1. 4-*O*-Phenylethyl-2,3,6-tri-*O*benzyl-α-D-galactopyranosyl-(1,1)-(2*S*,3*S*,4*R*)-2-azido-3,4-di-*O*-benzyl-octadecan-1,3,4-triol (8)

As shown in Scheme 4, a solution of alcohol **6** (114 mg, 0.12 mmol) and 2-phenylethyl iodide (0.17 mL, 1.2 mmol) in dry DMF (2 mL) was treated with Ag_2O (220 mg, 0.95 mmol) at 90 °C for 10 h. After cooled to room temperature, the mixture was diluted with ethyl acetate (10 mL), washed twice with water and then brine. The organic layer was dried over anhydrous Na_2SO_4, filtered and concentrated in vacuo. The residue was purified by column chromatography with hexane/ethyl acetate (15:1) to give 24 mg of product in 19% yield and recover 83 mg of compound **6**. HRMS calcd for $C_{67}H_{83}N_3O_8Na$ ($[M+Na]^+$) 1082.6229, found 1082.6257.

5.5.2. Ar2-GSL

Triphenylphosphine (8 mg, 0.030 mmol) was added to a solution of azide **8** (20 mg, 0.018 mmol) in benzene (3 mL) and water (0.1 mL). The reaction mixture was stirred at 50 °C for 10 h. The solvent was evaporated under reduced pressure and azeotroped with benzene (2 × 10 mL). Then it was dissolved in dry THF (2 mL) and treated with cerotic acid (8 mg, 0.020 mmol) and EDCI (4 mg, 0.020 mmol). After stirring for 10 h at room temperature, the solvent was evaporated and the residue was partitioned between CH_2Cl_2 (10 mL) and water (10 mL). The organic layer was separated and dried over Na_2SO_4. After concentrated, the residue was purified by silica gel flash chromatography (1:4 EtOAc–hexane) to provide 14 mg of product.

A suspension of the above product (14 mg, 0.01 mmol) and 5 mg of $Pd(OH)_2$ in $EtOH/CH_2Cl_2$ (3:1, 2 mL) was shaken for 4 h under H_2 atmosphere (40 psi). The catalytic Pd/C was filtered off through a Celite pad and the filtrate was concentrated to give 6 mg of product as powder in 35% yield for three steps. HRMS calcd for $C_{58}H_{107}NO_9Na$ ($[M+Na]^+$) 984.7838, found 984.7806.

5.6. Preparation of Ar3-GSL

5.6.1. 4-*O*-Phenylpropyl-2,3,6-tri-*O*benzyl-α-D-galactopyranosyl-(1,1)-(2*S*,3*S*,4*R*)-2-azido-3,4-di-*O*-benzyl-octadecan-1,3,4-triol (9)

As shown in Scheme 5, a solution of alcohol **6** (126 mg, 0.13 mmol) in dry DMF (2 mL) was treated with 60% NaH (8 mg,

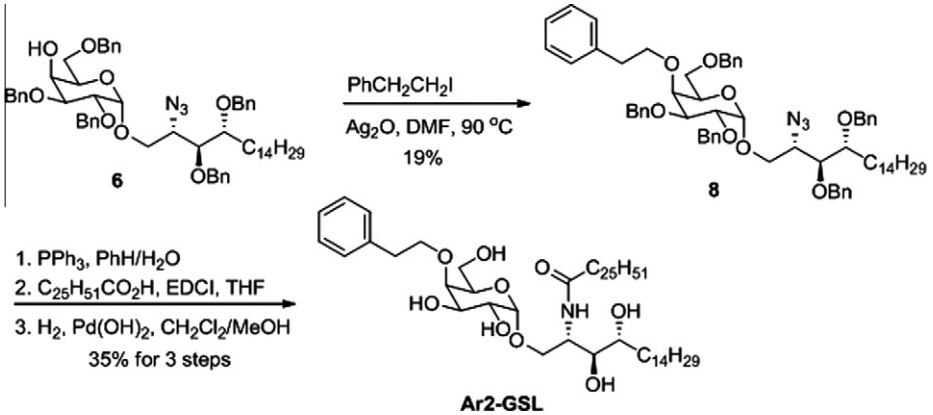

Scheme 4. Preparation of Ar2-GSL.

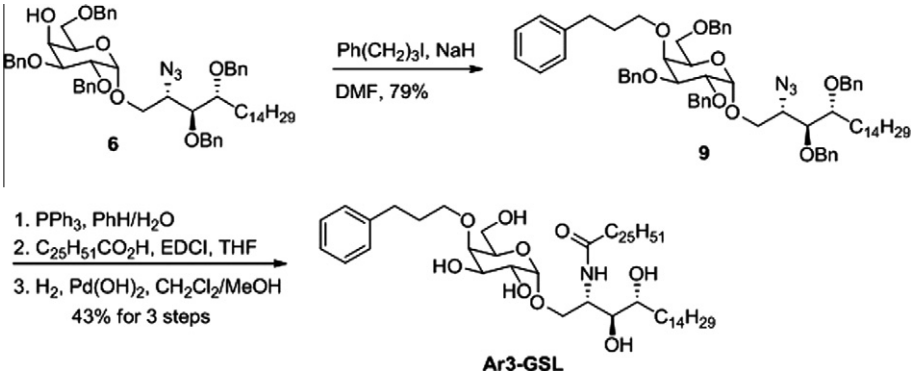

Scheme 5. Preparation of Ar3-GSL.

0.30 mmol) for 30 min. 3-Iodopropylbenzene (30 μL, 0.18 mmol) was added via syringe. The resulting mixture was stirred overnight. After diluted with ethyl acetate (10 mL), the mixture was washed twice with water and then brine. The organic layer was dried over anhydrous Na_2SO_4, filtered and concentrated in vacuo. The residue was purified by column chromatography with hexane/ethyl acetate (15:1) to give 111 mg of product in 79% yield. ^{1}H NMR (500 MHz, $CDCl_3$) δ 7.39–7.17 (m, 30H), 4.94 (d, J = 3.3 Hz, 1H), 4.48 (d, J = 12.1 Hz, 1H), 4.81 (d, J = 12.1 Hz, 1H), 4.74–4.69 (m, 3H), 4.66 (d, J = 11.4 Hz, 1H), 4.61 (d, J = 11.5 Hz, 1H), 4.54 (d, J = 8.8 Hz, 1H), 4.51 (d, J = 8.5 Hz, 1H), 4.46 (d, J = 11.8 Hz, 1H), 4.06–4.02 (m, 2H), 4.01–3.92 (m, 3H), 3.83 (m, 1H), 3.78–3.75 (m, 3H), 3.70–3.64 (m, 2H), 3.56–3.50 (m, 2H), 2.67 (t, J = 7.7 Hz, 2H), 1.90 (m, 2H), 1.70 (m, 1H), 1.58 (m, 1H), 1.44 (m, 1H), 1.36–1.26 (m, 23H), 0.93 (t, J = 6.9 Hz, 3H); ^{13}C NMR (125 MHz, $CDCl_3$) δ 142.2, 138.83, 138.80, 138.5, 138.2, 138.0, 128.5, 128.41, 128.36, 128.30, 128.28, 128.25, 127.9, 127.8, 127.71, 127.68, 127.59, 127.50, 127.45, 127.41, 125.68, 98.8, 79.4, 79.0, 78.7, 76.3, 75.8, 73.7, 73.5, 73.3, 72.9, 72.7, 72.1, 69.7, 68.8, 68.5, 62.0, 32.4, 32.0, 31.9, 30.0, 29.8, 29.74, 29.69, 29.67, 29.65, 29.4, 25.5, 22.7, 14.1; HRMS calcd for $C_{68}H_{87}N_3O_8Na$ ([M+Na]$^+$) 1096.6385, found 1096.6369.

5.6.2. Ar3-GSL

Triphenylphosphine (10 mg, 0.040 mmol) was added to a solution of azide **9** (35 mg, 0.033 mmol) in benzene (3 mL) and water (0.1 mL). The reaction mixture was stirred at 50 °C for 10 h. The solvent was evaporated under reduced pressure and azeotroped with benzene (2 × 10 mL). Then it was dissolved in dry THF (2 mL) and treated with cerotic acid (14 mg, 0.035 mmol) and EDCI (7 mg, 0.037 mmol). After stirring for 10 h at room temperature, the solvent was evaporated and the residue was partitioned between CH_2Cl_2 (10 mL) and water (10 mL). The organic layer was separated and dried over Na_2SO_4. After concentrated, the residue was purified by silica gel flash chromatography (1:3 EtOAc–hexane) to provide 26 mg of product.

A suspension of the above product (26 mg, 0.018 mmol) and 6 mg of $Pd(OH)_2$ in EtOH/CH_2Cl_2 (3:1, 3 mL) was shaken for 4 h under H_2 atmosphere (40 psi). The catalytic Pd/C was filtered off through a Celite pad and the filtrate was concentrated to give 14 mg of product as powder in 43% yield for three steps. HRMS calcd for $C_{59}H_{109}NO_9Na$ ([M+Na]$^+$) 998.7995, found 998.8012.

5.7. NKT hybridoma stimulation assay

As described before,[51] 100,000 A20/CD1 cells was pulsed overnight by the glycolipid compounds at different concentrations (1000 ng mL^{-1}, 100 ng mL^{-1}, 10 ng mL^{-1} and 1 ng mL^{-1}) in a total volume of 100 μL. After washed with medium, the pulsed A20/CD1 cells were mixed with 50,000 hybridoma cells and co-cultured in total volume of 200 μL. The supernatant was collected for IL-2 ELISA after another 24–48 h as described.[51]

5.8. Plate-bound CD1d presenting assay

The assay was carried out according to previous published procedure.[52] First, each well of the 96-well plate was coated by 0.5 μg mice CD1d protein (BD Pharmingen, CA, USA) in 100 μL pH 7.4 PBS at 37 °C for 2 h. Glycolipid antigens in gradient concentrations (1000, 100, 10, and 1 ng/mL in total volume of 100 μL) were then incubated in the coated wells for 24 h. After washing out the compounds, 1.0×10^5 NKT hybridoma cells was cultured in each treated well for 24 h. The supernatant was collected and the IL-2 concentration was measured by ELISA as described.

5.9. In vitro splenocytes stimulation assay

Fresh extracted spleens from 6 week C57BL/6 mice were grinded down to single cell suspension. For each well, 1.0×10^6 cells were cultured with glycolipid antigen at different concentrations as indicated in a 200 μL total volume. The mixtures were cultured for 72 h at 37 °C before the supernatants were collected. The IFN-γ and IL-4 concentration in the supernatants was measured by ELISA.

5.10. In vivo cytokine stimulation

All the animal housing and handling procedures were executed according to the animal usage protocol approved by The Ohio State University. Male C57BL/6 mice (4–6 weeks, The Jackson Laboratory, Maine, USA) were used here. The compounds were diluted to 10 μg/mL in PBS from the stock solution and 5 μg of each analogue was intravenously injected through the mouse tail vein, three mice a group. At each time point (Starting point, 2, 4, 6, and 24 h after injection), blood samples were collected from each mouse. The serum was separated and the IFN-γ and IL-4 concentrations in the serum were measured by ELISA.

5.11. Computer modeling and simulation

The crystal structures of both human and mouse CD1D (hCD1d and mCD1d) proteins presenting α-GalCer to their respective NKT-TCR proteins were retrieved from the Protein Databank,[53] PDB ID# 2PO6 and 3HE6, respectively. The crystal structures were aligned and a new complex was built using the iNKT-TCR protein from 2PO6 and the mCD1d/α-GalCer from 3HE6. This new complex underwent an energy minimization using Schrödinger's Macromodel software (Schrödinger, USA). The environment in which the minimization was performed involved the OPLS_20005[54]

forcefield in a solvent of water with a constant dielectric of 1.0, and the actual minimization parameters used the Low-memory Broyden-Fletcher-Goldfarb-Shanno (LBFGS) method[55] with maximum iterations of 500 converging on the gradient with a threshold of 0.05. The α-GalCer ligand in mCD1d/α-GalCer/TCR complex was then modified to form the ligands Ar1-GSL, Ar2-GSL, and Ar3-GSL, thereby yielding a total of four complexes. An additional energy minimization using the same parameters were performed in each of the systems. The mCD1d/Ar2-GSL and Ar3-GSL/NKT complexes then underwent 200 ps of molecular dynamics simulations in the same save environment with the OPLS_2005 forcefield.

Acknowledgments

This work was supported by National Institutes of Health R21AI083513 (P.G.W.) and State Key Laboratory of Phytochemistry & Plant Resources in West China (C.X). The authors thank Dr. Mitchell Kronenberg (LIAI, La Jolla, CA, USA) for providing us the A20/CD1cells and hybridoma cell lines.

References and notes

1. Kronenberg, M.; Gapin, L. *Nat. Rev. Immunol.* **2002**, *2*, 557.
2. Kronenberg, M. *Annu. Rev. Immunol.* **2005**, *23*, 877.
3. Bendelac, A.; Savage, P. B.; Teyton, L. *Annu. Rev. Immunol.* **2007**, *25*, 297.
4. Brigl, M.; Brenner, M. B. *Annu. Rev. Immunol.* **2004**, *22*, 817.
5. Borg, N. A.; Wun, K. S.; Kjer-Nielsen, L.; Wilce, M. C.; Pellicci, D. G.; Koh, R.; Besra, G. S.; Bharadwaj, M.; Godfrey, D. I.; McCluskey, J.; Rossjohn, J. *Nature* **2007**, *448*, 44.
6. Gadola, S. D.; Zaccai, N. R.; Harlos, K.; Shepherd, D.; Castro-Palomino, J. C.; Ritter, G.; Schmidt, R. R.; Jones, E. Y.; Cerundolo, V. *Nat. Immunol.* **2002**, *3*, 721.
7. Martin, L. H.; Calabi, F.; Lefebvre, F. A.; Bilsland, C. A. G.; Milstein, C. *Proc. Natl. Acad. Sci. U.S.A.* **1987**, *84*, 9189.
8. Martin, L. H.; Calabi, F.; Milstein, C. *Proc. Natl. Acad. Sci. U.S.A.* **1986**, *83*, 9154.
9. Calabi, F.; Milstein, C. *Nature* **1986**, *323*, 540.
10. Calabi, F.; Jarvis, J. M.; Martin, L.; Milstein, C. *Eur. J. Immunol.* **1989**, *19*, 285.
11. Natori, T.; Koezuka, Y.; Higa, T. *Tetrahedron Lett.* **1993**, *34*, 5591.
12. Natori, T.; Morita, M.; Akimoto, K.; Koezuka, Y. *Tetrahedron* **1994**, *50*, 2771.
13. Morita, M.; Motoki, K.; Akimoto, K.; Natori, T.; Sakai, T.; Sawa, E.; Yamaji, K.; Koezuka, Y.; Kobayashi, E.; Fukushima, H. *J. Med. Chem.* **1995**, *38*, 2176.
14. Shimosaka, A. *Int. J. Hematol.* **2002**, *76*, 277.
15. Naumov, Y. N.; Bahjat, K. S.; Gausling, R.; Abraham, R.; Exley, M. A.; Koezuka, Y.; Balk, S. B.; Strominger, J. L.; Clare-Salzer, M.; Wilson, S. B. *Proc. Natl. Acad. Sci. U.S.A.* **2001**, *98*, 13838.
16. Taniguchi, M.; Seino, K.-i.; Nakayama, T. *Nat. Immunol.* **2003**, *4*, 1164.
17. Nakagawa, R.; Serizawa, I.; Motoki, K.; Sato, M.; Ueno, H.; Iijima, R.; Nakamura, H.; Shimosaka, A.; Koezuka, Y. *Oncol. Res.* **2000**, *12*, 51.
18. Fuji, N.; Ueda, Y.; Fujiwara, H.; Toh, T.; Yoshimura, T.; Yamagishi, H. *Clin. Cancer Res.* **2000**, *6*, 3380.
19. Kobayashi, E.; Motoki, K.; Uchida, T.; Fukushima, H.; Koezuka, Y. *Oncol. Res.* **1995**, *7*, 529.
20. Forestier, C.; Takaki, T.; Molano, A.; Im, J. S.; Baine, I.; Jerud, E. S.; Illarionov, P.; Ndonye, R.; Howell, A. R.; Santamaria, P.; Besra, G. S.; DiLorenzo, T. P.; Porcelli, S. A. *J. Immunol.* **2007**, *178*, 1415.
21. Chen, Y.-G.; Choisy-Rossi, C.-M.; Holl, T. M.; Chapman, H. D.; Besra, G. S.; Porcelli, S. A.; Shaffer, D. J.; Roopenian, D.; Wilson, S. B.; Serreze, D. V. *J. Immunol.* **2005**, *174*, 1196.
22. Hong, S.; Wilson, M. T.; Serizawa, I.; Wu, I.; Singh, N.; Naidenko, O. V.; Miura, T.; Haba, T.; Scherer, D. C.; Wei, J.; Kronenberg, M.; Koezuka, Y.; Van Kaer, L. *Nat. Med.* **2001**, *7*, 1052.
23. Sharif, S.; Arreaza, G. A.; Zucker, P.; Mi, Q.-S.; Sondhi, J.; Naidenko, O. V.; Kronenberg, M.; Koezuka, Y.; DeLovitch, T. L.; Gombert, J.-M.; Leite-de-Moraes, M.; Gouarin, C.; Zhu, B.; Hameg, A.; Nakayama, T.; Taniguchi, M.; LePault, F.; Lehuen, A.; Bach, J.-F.; Herbelin, A. *Nat. Med.* **2001**, *7*, 1057.
24. Kakimi, K.; Guidotti, L. G.; Koezuka, Y.; Chisari, F. V. *J. Exp. Med.* **2000**, *192*, 921.
25. Nieuwenhuis, E. E. S.; Matsumoto, T.; Exley, M.; Schleipman, R. A.; Glickman, J.; Bailey, D. T.; Corazza, N.; Colgan, S. P.; Onderdonk, A. B.; Blumberg, R. S. *Nat. Med.* **2002**, *8*, 588.
26. Hazlett, L. D.; Li, Q.; Liu, J.; McClellan, S.; Du, W.; Barrett, R. P. *J. Immunol.* **2007**, *179*, 1138.
27. Giaccone, G.; Punt Cornelis, J. A.; Ando, Y.; Ruijter, R.; Nishi, N.; Peters, M.; von Blomberg, B. M. E.; Scheper Rik, J.; van der Vliet, H. J. J.; van den Eertwegh, A. J. M.; Roelvink, M.; Beijnen, J.; Zwierzina, H.; Pinedo Herbert, M. *Clin. Cancer Res.* **2002**, *8*, 3702.
28. Crul, M.; Mathot, R. A. A.; Giaccone, G.; Punt, C. J. A.; Rosing, H.; Hillebrand, M. J. X.; Ando, Y.; Nishi, N.; Tanaka, H.; Schellens, J. H. M.; Beijnen, J. H. *Cancer Chemother. Pharmacol.* **2002**, *49*, 287.
29. Veldt, B. J.; van der Vliet, H. J. J.; von Blomberg, B. M. E.; van Vlierberghe, H.; Gerken, G.; Nishi, N.; Hayashi, K.; Scheper, R. J.; de Knegt, R. J.; van den Eertwegh, A. J. M.; Janssen, H. L. A.; van Nieuwkerk, C. M. J. *J. Hepatol.* **2007**, *47*, 356.
30. Parekh, V. V.; Wilson, M. T.; Olivares-Villagomez, D.; Singh, A. K.; Wu, L.; Wang, C. R.; Joyce, S.; Van Kaer, L. *J. Clin. Invest.* **2005**, *115*, 2572.
31. Uldrich, A. P.; Crowe, N. Y.; Kyparissoudis, K.; Pellicci, D. G.; Zhan, Y.; Lew, A. M.; Bouillet, P.; Strasser, A.; Smyth, M. J.; Godfrey, D. I. *J. Immunol.* **2005**, *175*, 3092.
32. Fujii, S.-i.; Shimizu, K.; Kronenberg, M.; Steinman, R. M. *Nat. Immunol.* **2002**, *3*, 867.
33. Nieda, M.; Okai, M.; Tazbirkova, A.; Lin, H.; Yamaura, A.; Ide, K.; Abraham, R.; Juji, T.; Macfarlane David, J.; Nicol Andrew, J. *Blood* **2004**, *103*, 383.
34. Ishikawa, A.; Motohashi, S.; Ishikawa, E.; Fuchida, H.; Higashino, K.; Otsuji, M.; Iizasa, T.; Nakayama, T.; Taniguchi, M.; Fujisawa, T. *Clin. Cancer Res.* **2005**, *11*, 1910.
35. Chang, D. H.; Osman, K.; Connolly, J.; Kukreja, A.; Krasovsky, J.; Pack, M.; Hutchinson, A.; Geller, M.; Liu, N.; Annable, R.; Shay, J.; Kirchhoff, K.; Nishi, N.; Ando, Y.; Hayashi, K.; Hassoun, H.; Steinman, R. M.; Dhodapkar, M. V. *Exp. Med.* **2005**, *201*, 1503.
36. Koch, M.; Stronge, V. S.; Shepherd, D.; Gadola, S. D.; Mathew, B.; Ritter, G.; Fersht, A. R.; Besra, G. S.; Schmidt, R. R.; Jones, E. Y.; Cerundolo, V. *Nat. Immunol.* **2005**, *6*, 819.
37. Zajonc, D. M.; Cantu, C.; Mattner, J.; Zhou, D.; Savage, P. B.; Bendelac, A.; Wilson, I. A.; Teyton, L. *Nat. Immunol.* **2005**, *6*, 810.
38. Wu, D.; Zajonc, D. M.; Fujio, M.; Sullivan, B. A.; Kinjo, Y.; Kronenberg, M.; Wilson, I. A.; Wong, C. H. *Proc. Natl. Acad. Sci. U.S.A.* **2006**, *103*, 3972.
39. Iijima, H.; Kimura, K.; Sakai, T.; Uchimura, A.; Shimizu, T.; Ueno, H.; Natori, T.; Koezuka, Y. *Bioorg. Med. Chem.* **1998**, *6*, 1905.
40. Zeng, Z. H.; Castano, A. R.; Segelke, B. W.; Stura, E. A.; Peterson, P. A.; Wilson, I. A. *Science* **1997**, *277*, 339.
41. Xia, C.; Zhang, W.; Zhang, Y.; Chen, W.; Nadas, J.; Severin, R.; Woodward, R.; Wang, B.; Wang, X.; Kronenberg, M.; Wang, P. G. *ChemMedChem* **2009**, *4*, 1810.
42. Zhou, X.-T.; Forestier, C.; Goff, R. D.; Li, C.; Teyton, L.; Bendelac, A.; Savage, P. B. *Org. Lett.* **2002**, *4*, 1267.
43. Kawano, T.; Cui, J.; Koezuka, Y.; Toura, I.; Kaneko, Y.; Motoki, K.; Ueno, H.; Nakagawa, R.; Sato, H.; Kondo, E.; Koseki, H.; Taniguchi, M. *Science* **1997**, *278*, 1626.
44. Wu, D.; Xing, G.-W.; Poles, M. A.; Horowitz, A.; Kinjo, Y.; Sullivan, B.; Bodmer-Narkevitch, V.; Plettenburg, O.; Kronenberg, M.; Tsuji, M.; Ho, D. D.; Wong, C.-H. *Proc. Natl. Acad.Sci. U.S.A.* **2005**, *102*, 1351.
45. Nadas, J.; Li, C.; Wang, P. G. *J. Chem. Inf. Model.* **2009**, *49*, 410.
46. Li, Y.; Girardi, E.; Wang, J.; Yu, E. D.; Painter, G. F.; Kronenberg, M.; Zajonc, D. M. *J. Exp. Med.* **2010**, *207*, 2383.
47. Sinnokrot, M. O.; Sherrill, C. D. *J. Am. Chem. Soc.* **2004**, *126*, 7690.
48. Zhao, Y.; Truhlar, D. G. *J. Chem. Theory Comput.* **2005**, *1*, 415.
49. Sidobre, S.; Naidenko, O. V.; Sim, B.-C.; Gascoigne, N. R. J.; Garcia, K. C.; Kronenberg, M. *J. Immunol.* **2002**, *169*, 1340.
50. Kinjo, Y.; Wu, D.; Kim, G.; Xing, G. W.; Poles, M. A.; Ho, D. D.; Tsuji, M.; Kawahara, K.; Wong, C. H.; Kronenberg, M. *Nature* **2005**, *434*, 520.
51. Zhang, W.; Zheng, X.; Xia, C.; Perali, R. S.; Yao, Q.; Liu, Y.; Zheng, P.; Wang, P. G. *ChemBioChem* **2008**, *9*, 1423.
52. Kinjo, Y.; Tupin, E.; Wu, D.; Fujio, M.; Garcia-Navarro, R.; Benhnia, M. R.-E.-I.; Zajonc, D. M.; Ben-Menachem, G.; Ainge, G. D.; Painter, G. F.; Khurana, A.; Hoebe, K.; Behar, S. M.; Beutler, B.; Wilson, I. A.; Tsuji, M.; Sellati, T. J.; Wong, C.-H.; Kronenberg, M. *Nat. Immunol.* **2006**, *7*, 978.
53. Berman, H. M.; Westbrook, J.; Feng, Z.; Gilliland, G.; Bhat, T. N.; Weissig, H.; Shindyalov, I. N.; Bourne, P. E. *Nucleic Acids Res.* **2000**, *28*, 235.
54. Jorgensen, W. L.; Tiradorives, J. *J. Am. Chem. Soc.* **1988**, *110*, 1657.
55. Head, J. D.; Zerner, M. C. *Chem. Phys. Lett.* **1985**, *122*, 264.